CONEM 2016
CONGRESSO NACIONAL DE ENGENHARIA MECÂNICA
21 - 25 AGOSTO DE 2016
FORTALEZA - CEARÁ

DYNAMICS AND CONTROL OF AN SMA-PENDULUM SYSTEM

Dimitri D. A. Costa, dda.costa@mecanica.coppe.ufrj.br[1]
Marcelo A. Savi, savi@mecanica.coppe.ufrj.br[1]

[1] Center for Nonlinear Mechanics, COPPE – Department of Mechanical Engineering, Universidade Federal do Rio de Janeiro, 21.941.972 – Rio de Janeiro – RJ, Brazil, P.O. Box 68.503

Abstract: *Pendulum systems are extensively analyzed due to a variety of reasons, being a source of motivation for several discoveries in nonlinear dynamics and other fields of engineering. Their simplicity and rich dynamics including bifurcations, chaos and transient chaos makes it a great choice for testing new ideas and control techniques. Smart materials represent a class of advanced materials with remarkable properties conferred by the coupling between different physical fields. Usually, they are employed for control purposes due to their adaptive capacity. Shape memory alloys (SMAs) belong to the smart materials class showing a broad use for numerous applications. This work deals with the nonlinear dynamics of an SMA-Pendulum system composed of a nonlinear pendulum coupled with SMA springs. A numerical investigation is carried out exploiting the temperature dependent behavior of the SMA. Complex responses are presented and the possibility of thermal control of the system is investigated. Nonlinear control techniques can be applied in order to change between different system responses.*

Key-words: *Bifurcation Analysis and Applications, Control of Chaos, Chaos and Global Nonlinear Dynamics.*

1. INTRODUCTION

Pendulum systems are extensively analysed due to a variety of reasons, being a source of motivation for several discoveries in nonlinear dynamics and other fields of engineering. De Paula *et al.* (2006) discussed some aspects of pendulum dynamics, presenting an experimental-numerical investigation of a typical mechanical apparatus. Results show several complex responses that include bifurcations, chaos and transient chaos. Nonlinear control of these systems are investigated in several references, and it should be highlighted the use of either fuzzy logic or chaos control approaches (Bessa *et al.* 2009; De Paula; Savi, 2009; Pan *et al.*, 2013). Pendulum-like systems are also employed to model biological systems as Suzuki *et al.* (2012) that models the control of an ankle. Motor systems are also treated as Chen *et al.* (2014) that discussed the control of induction motors for electrical vehicles. These systems are also used to model cranes and their swings according to the work of Ju *et al.* (2006).

Smart materials represent a class of advanced materials with remarkable properties conferred by the coupling between different physical fields. Usually, they are employed in control due to their adaptive capacity. Shape memory alloys (SMAs) belong to this type of materials, having interesting properties for applied dynamics (Savi, 2015) being widely applied in vibration control (Bessa *et al.*, 2013), origami structures (Kuribayashi *et al.*, 2006), robotics (Kim *et al.*, 2006) and energy harvesting (Lebedev *et al.*, 2011), showing a broad use and potential for numerous applications. Their unique behaviour is due to the thermoelastic martensitic transformations that imply some of their traditional effects as pseudoelasticity and shape memory effect. The first one is identified as a complete strain recovery of the material with a large hysteresis in a loading-unloading cycle. On the other hand, shape memory effect is the ability to completely recover an amount of residual strain after a proper themomechanical loading process. These characteristics can be used to mimic biological movements, robotics, aerospace engineering, shape and vibration control, among others (Kim *et al.*, 2006; Kuribayashi *et al.*, 2006; Lebedev *et al.*, 2011; Machado; Savi, 2003; Machado *et al.*, 2003). Synergistic use of smart materials has been increasing, by exploring the proper characteristics of each material involved. SMA-piezoelectric structures are good examples for enhance energy harvesting capacity combining different characteristics of smart materials (Lebedev *et al.*, 2011; Arrieta *et al.*, 2010; Silva *et al.*, 2015).

This work deals with the nonlinear dynamics of an SMA-Pendulum system composed of a nonlinear pendulum coupled with SMA springs. This system has adaptive behaviour, presenting a temperature dependent response. Dynamical investigation is carried out pointing to some advantages of the use of SMA elements as well as some possible control applications. Time delay feedback control is applied showing an important potential application.

2. SMA-PENDULUM SYSTEM

The pendulum consists of a disc with diameter D with a lump mass m. The excitation of the pendulum is provided by a DC motor, with an arm of length b, connected to string-spring system. A magnetic device provides dissipation to the system. The system is similar to the one discussed by De Paula *et al.* (2006) except that SMA springs are used for the excitation mechanism (Fig. 1).

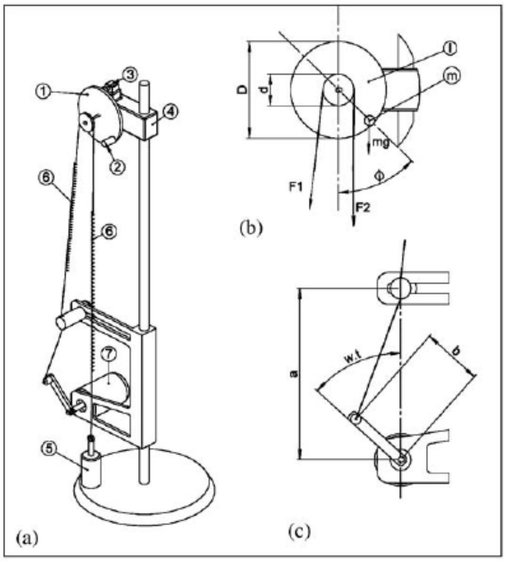

Figure 1: Nonlinear pendulum: a) physical model (1) metallic disc; (2) lumped mass; (3) magnetic damping device; (4) rotary motion sensor; (5) anchor; (6) SMA spring; (7) electric motor; b) Parameters and forces on the metallic disc; c) Parameters for driving device (De Paula *et al.*, 2006)**.**

By considering that ϕ is the angle of the pendulum, and assuming that dissipation is a combination of linear viscous and dry friction, respectively represented by coefficients ϑ and μ, the equation of motion is given by

$$\phi'' = -\frac{\vartheta}{Iw_0}\phi' - \frac{\mu}{mgD}\,\mathrm{sign}(\phi') - \frac{\sin(\phi)}{2} + \frac{d}{2mgD}(F_m - s_m) \tag{1.1}$$

Where a is the distance between the center of the disc and the center of the rotor, I is the angular inertia of the pendulum, g is the acceleration of gravity, ω_0 is a reference frequency defined as follows:

$$\omega_0 = \sqrt{\frac{mgd}{I}} \tag{1.2}$$

Time derivative ( )' is related to dimensionless time, t^*, defined by $t^* = t\omega_0$. Moreover, s_m is the force of the anchored spring and F_m is the excitation force of the spring and motor system.

The geometric displacement due to the movement of the motor can be given as:

$$y = \sqrt{\left(a^2 + b^2 - 2ab\cos\left(\frac{\omega t^*}{w_0} + \theta\right)\right)} - (a - b) - \frac{d\phi}{2} \tag{2}$$

Where θ is the initial phase of the motor, ω is the excitation frequency and b is the motor arm length.

Different models are proposed to describe the thermomechanical behavior of SMAs (Aguiar *et al.*, 2010; Lagoudas, 2008; Paiva *et al.*, 2005), and specifically for springs (Aguiar *et al.*, 2010; Enemark *et al.*, 2016). Among all these descriptions polynomial models are the simplest alternative that capture the general thermomechanical behavior of SMAs, being interesting to be employed for the qualitative description of dynamical systems. To this work a stress-strain (σ-ε) relation is adopted as follows:

$$\sigma = a_m^*(T - T_M)\varepsilon - b_m^*\varepsilon^3 + \frac{{b_m^*}^2}{a_m^*(T_A - T_M)}\varepsilon^5 \tag{3}$$

Where a_m^* and b_m^* are material parameters, T_M is the temperature below which only martensitic phase is stable, T_A is the temperature above which only austenitic phase is stable (at stress free scenario), T is the temperature. Based on that, and assuming that phase transformation is homogeneous for the spring cross-section, it is possible to write a force-displacement equation for the spring that is formally similar to this stress-strain expression (Aguiar *et al.*, 2010). Hence,

$$F_m = a_m(T - T_M)y - b_m y^3 + \frac{{b_m}^2}{a_m(T_A - T_M)}y^5 \tag{4.1}$$

$$s_m = a_m(T - T_M)\frac{\phi d}{2} - b_m\left(\frac{\phi d}{2}\right)^3 + \frac{{b_m}^2}{a_m(T_A - T_M)}\left(\frac{\phi d}{2}\right)^5 \tag{4.2}$$

3. NUMERICAL SIMULATIONS

Numerical simulations are performed to investigate the nonlinear dynamics of the SMA-pendulum system. Fourth-order Runge-Kutta method is employed and Lyapunov exponents are calculated using the algorithm proposed by Wolf et al. (1985). Employed parameters are the following: $m = 1.47$ kg, $D = 9.5$ cm, $d = 4.8$ cm, $b = 6$ cm, $a = 16$ cm, $\mu = 1.272\ 10^{-4}$ Nm, $\vartheta = 2.368\ \frac{kgm^2}{s}$, $g = 9.81\ m/s^2$. SMA parameters are adjusted with experimental data: $T_A = 289.35$ K, $T_M = 282.45$ K, $a_m = 0.4375$ N/mK and $b_m = 150$ Pa/m.

Initially, the structure of equilibrium points is analysed, giving special attention to its temperature dependent behaviour. In this regard, the system is not subjected to excitation and therefore, the motor is at rest in a specific angle θ. A locus of equilibrium points against the forcing motor phase is plotted on three different temperatures: one under T_M, one in between T_M and T_A and one above T_A. The stability of each equilibrium point is analysed assessing the eigenvalues of the Jacobian matrix. A reference situation is defined at high temperature where results are similar to the one obtained with an elastic spring as discussed in (De Paula *et al.*, 2006). This situation is simulated considering T = 291.15 K. Figure 2 shows the equilibrium point locus for this case presenting regions related to just only one stable equilibrium point and a region ($2.71 \leq \theta \leq 4.11$) related to three equilibrium points (two stable and one unstable).

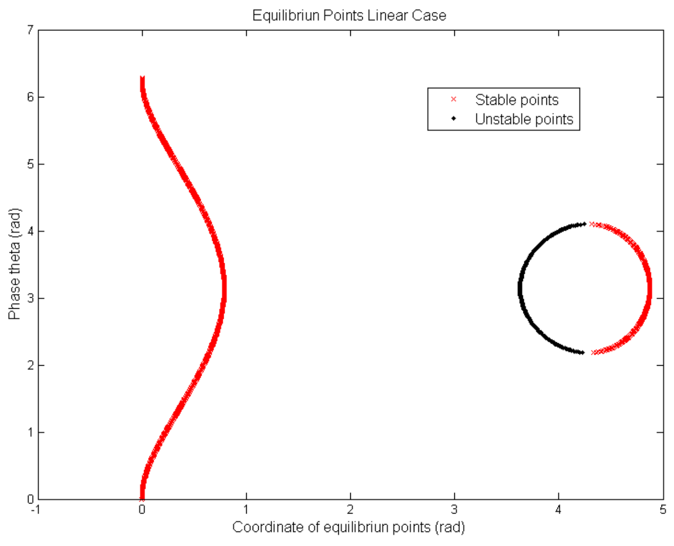

Figure 2: Location of equilibrium points in rad against forcing motor phase in rad for the linear case.

The introduction of SMA springs promotes dramatic changes on the system behaviour. Figure 3 show the situation where $T < T_M$. There are five equilibrium points for $\theta = 0$, two of them unstable and three stable, all positioned symmetrically around the origin. The symmetry of the system is broken by changing the motor phase, which moves the equilibrium points until a stable and an unstable equilibrium points collide. We emphasize here that asymmetries are always introduced by the motor's phase angle θ. The further increase of temperature changes the structure of equilibrium points. This intermediate temperature range ($T_M < T < T_A$) allows both martensite and austenite to be stable and therefore, is related to a greater equilibrium point structure. This can be seen clearly on Fig. 4 where the previous ellipse of Fig. 3 is now two separated paths of equilibrium points, also another ellipse appears. A new dramatic change occurs when temperature values approach T_A. After this point, only austenite is stable in a stress-free state. At this stage the ellipse structures start to contract and form by the coalescences of stable and unstable paths of equilibrium points. Here is important to notice that the ellipses can be formed as single, pairs or divide them while collapsing (Fig.

5). This ellipse division is unique to the non-linear effects of the SMA-pendulum system and would not appear in any linear case. The limit case occurs at $T = 291.15$ K where constitutive nonlinearity can be neglected and the original case presented in Fig. 2 is reproduced.

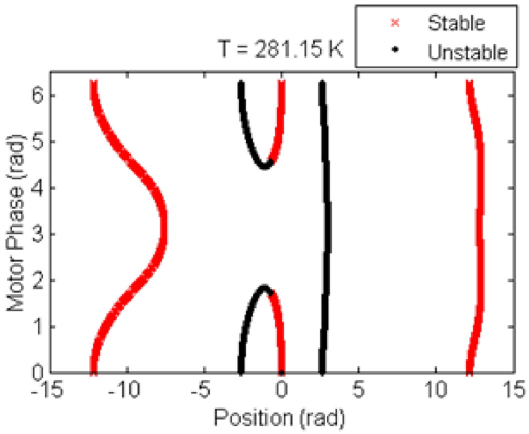

Figure 3: Location of equilibrium points in rad against forcing motor phase in rad for the SMA spring on temperatures below T_m.

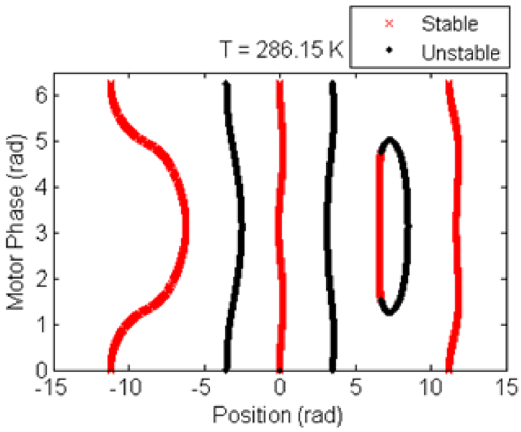

Figure 4: Location of equilibrium points in rad against forcing motor phase in rad for the SMA spring system case on $T_m < T < T_A$.

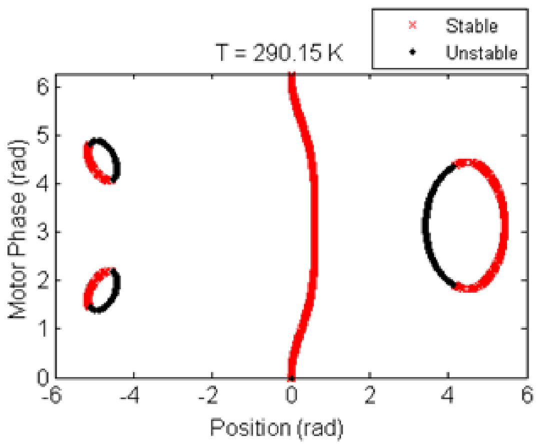

Figure 5: Location of equilibrium points in rad against forcing motor phase in rad for the SMA spring system case on $T > T_A$.

Forced vibration of the system is now focused. Bifurcations diagrams are initially investigated providing a general comprehension about the system dynamics. Figure 6 presents a bifurcation diagram showing the position under temperature variation considering forcing frequency of ω = 5.5 rad/s. Diagrams are constructed by simulating 30 different initial conditions and eliminating the first 600 periods of each simulation. Note that the change on temperature causes various kinds of responses. Periodic and chaotic responses are possible and multistability can also be observed since different initial conditions are related to different solutions. In this regard, it is important to notice the coexistence of period-1 and chaotic response when T = 291.15 K (Fig. 7) and of a period-12 and a period-1 response (Fig. 8) when T = 283.55. It is also relevant to notice that there is a periodic window around 291.15 K for the P2 and P3 initial conditions while the system initialized at P1 still presents an chaotic response in the region (in detail on Fig. 6).

The influence of frequency variation is verified by considering a bifurcation diagram with constant temperature, T = 291.15 K (Fig. 9). Once again, multiple chaotic regions are observed coexisting with period-1 solutions: three small chaotic-like twin regions around 4.78 rad/s, 5.18 rad/s and 5.5 rad/s, and two great chaotic region near 5.4 rad/s and 6 rad/s. Differences on these chaotic regions suggest that their attractors have different structures and properties.

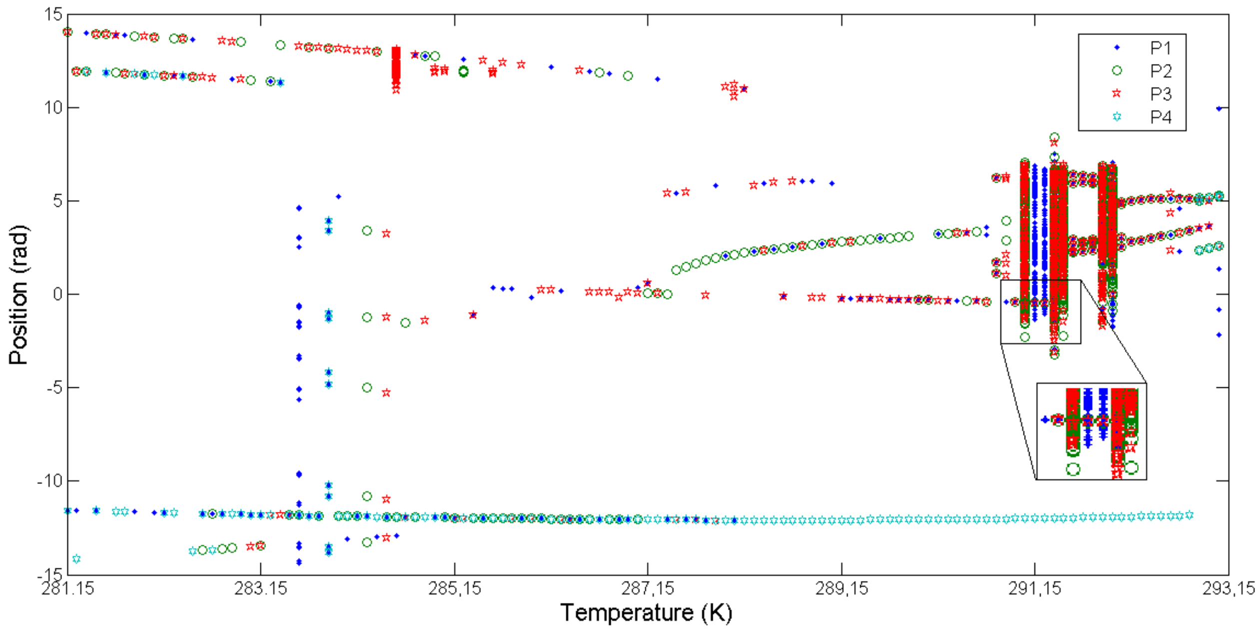

Figure 6: Bifurcation diagram for ω = 5.5 rad/s. Only the results of the most relevant points are shown for simplicity, other initial condition only presents the same trends of the other 4.

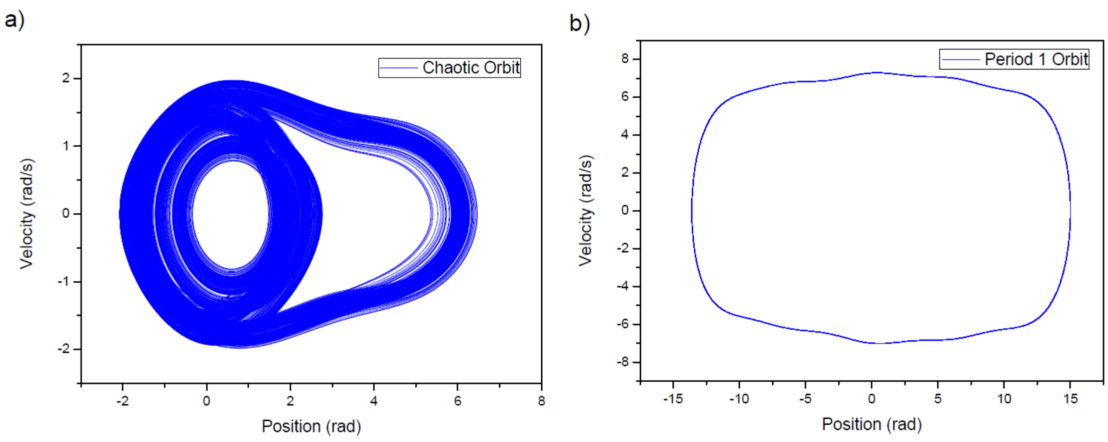

Figure 7: Orbits at forcing frequency of 5.5 rad/s and T=291.15 K. a) Chaotic, b) Periodic.

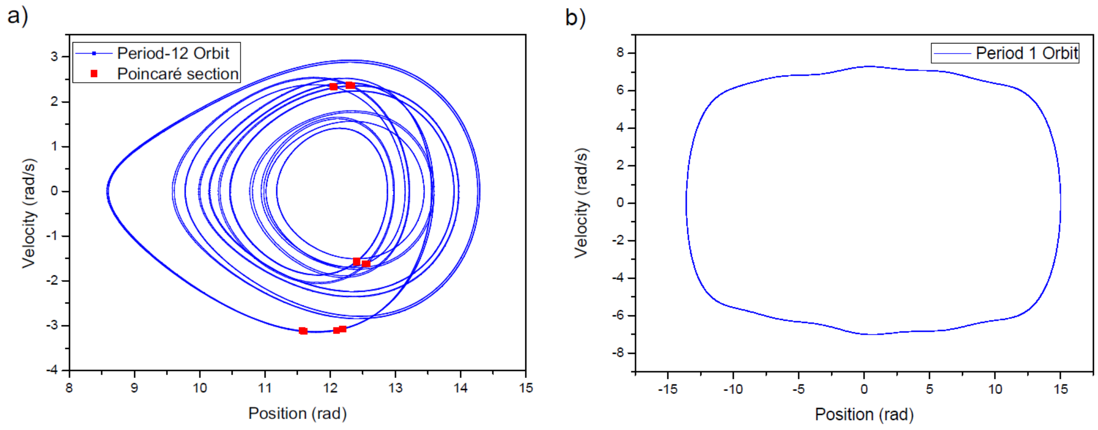

Figure 8: Orbits at forcing frequency of 5.5 rad/s and T=291.15 K. a) Period-12 note that each read marker of the Poincare section is in fact two markers right next to each other, b) Period-1.

Some specific solutions on the bifurcation diagram, shown on figure 9, are now analyzed. Figure 10a presents a period-2 response for the forcing frequency of 3.59 rad/. Figure 10b presents a period-1 response with ω = 5.1 rad/s. By considering ω = 5.5 rad/s a chaotic response appears. Figure 11 shows both phase space and Poincaré map of this response that can be assured as chaotic by calculating the Lyapunov exponents using the algorithm proposed by Wolf *et al.* (1985) that presents a positive largest value (λ = 0.14±0.02 bit/s). Poincaré section shows a three region disconnected fractal-like structure. Figure 10 presents similar chaotic response considering ω = 4.78 rad/s but with a two-region attractor instead of three-region as the previous case. The period-1 orbits that coexist with chaotic regions have the form of the orbits on figure 8b and figure 10b.

Transient chaos is a chaotic response associated with a chaotic saddle while chaos is related to a chaotic attractor. The essential difference is that chaotic saddle is expelling the solution and therefore, the system presents a transient response instead of a permanent chaos. Analysis of this kind of response is difficult as the transient chaos have a limit number of cycles before turning into periodic motion. Figure 13 presents the transient chaos showing the chaotic saddle and the time history of the response with ω = 6 rad/s, it was created by find an initial condition which allows the solution to be in the chaotic saddle for a great number of periods. The fractal-like structure of the chaotic saddle is highlighted as is the positive Lyapunov exponent related to it (0.52±0.03 bits/s).

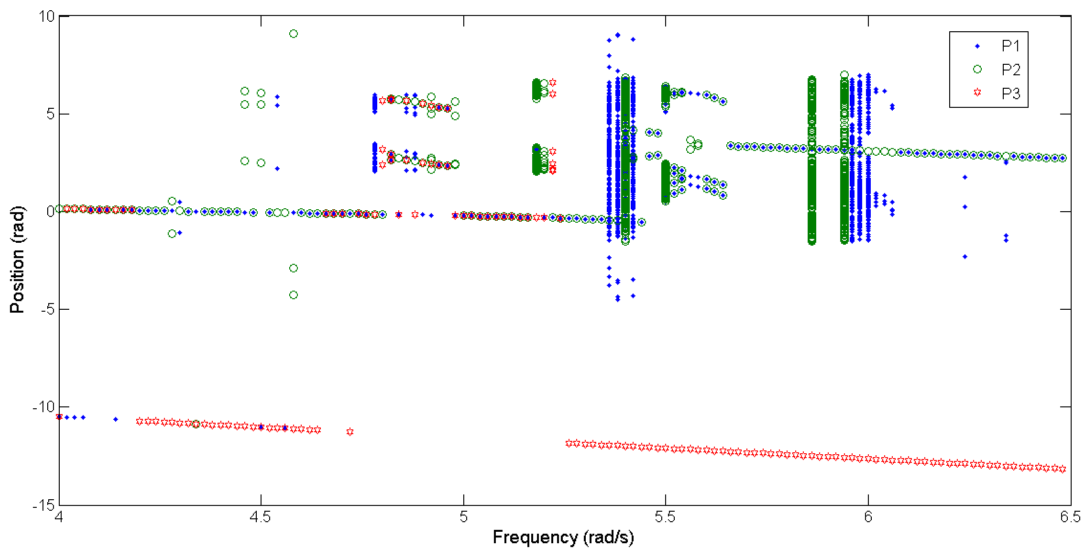

Figure 9: Bifurcation diagram varying the forcing frequency for T = 291.15 K. Only the results of the most relevant points are shown for simplicity, other initial condition only presents the same trends of the other 3.

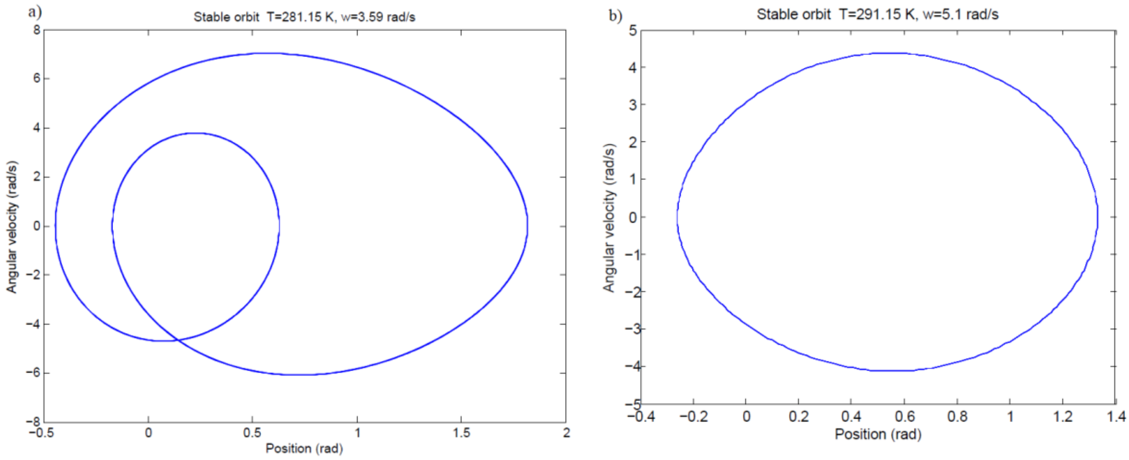

Figure 10: System solutions on different forcing frequencies. a) 3.59 rad/s; b) 5.1 rad/s.

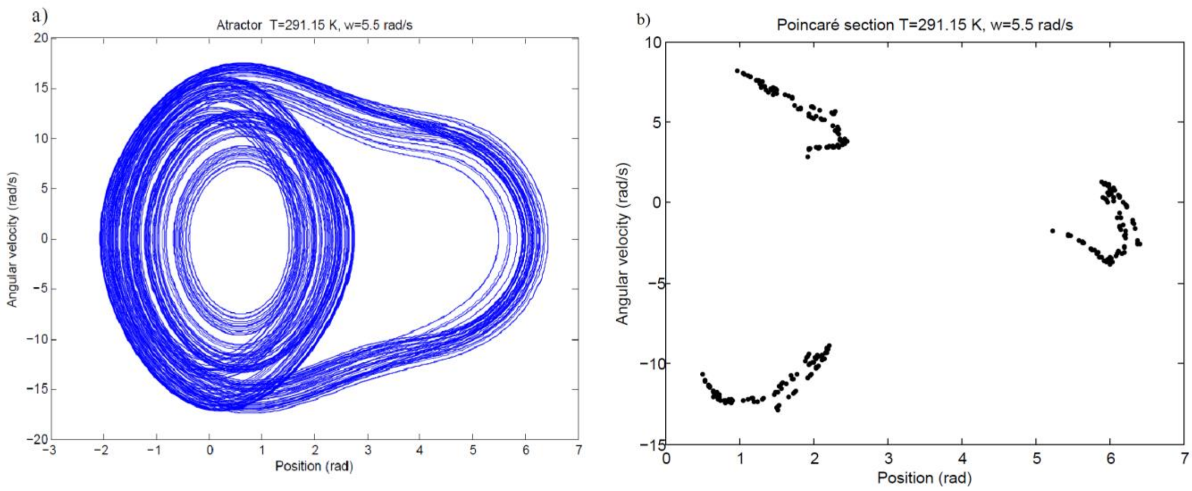

Figure 11: Chaotic solution with ω = 5.5 rad/s. a) Phase space. b) Poincaré section.

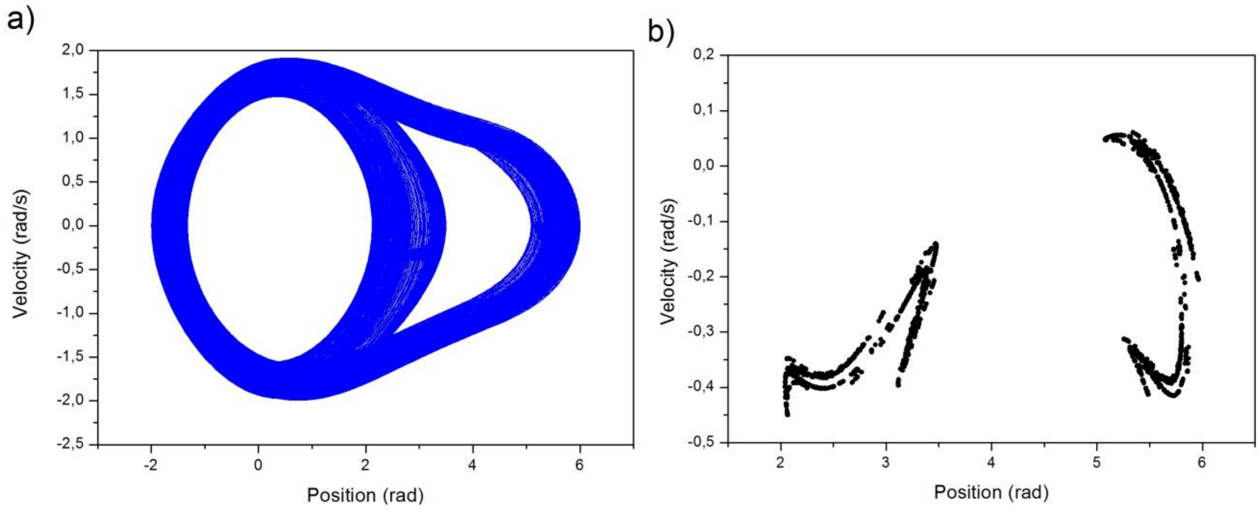

Figure 12: Chaotic solution with ω = 4.78 rad/s. a) Phase space. b) Poincaré section.

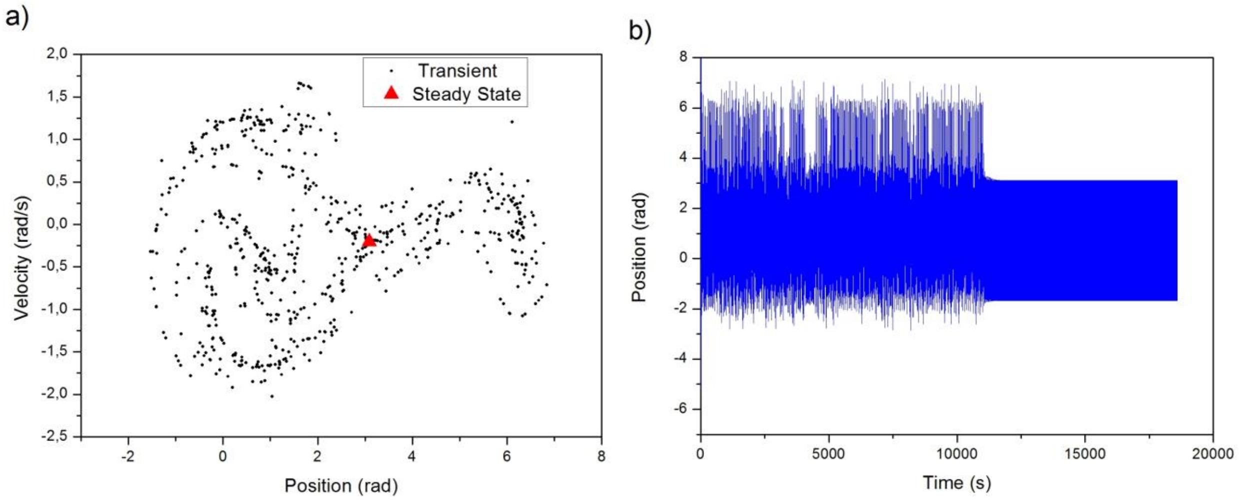

Figure 13: Transient chaos ω = 6 rad/s, initial conditions (10.152 rad, 0 rad/s). a) Chaotic saddle and steady state. b) Time history.

The use of SMA system is interesting especially for control purposes. Based on that, a feedback control is employed assuming that:

$$\dot{x} = f(x) + K(x_\tau - x) \tag{5}$$

where x is the present state of the system, x_τ is delayed state of the system on a delayed time τ, K is a gain matrix always positive. This control method was first proposed in (PYRAGAS, 1992) to stabilize unstable periodic orbits in chaotic responses.

Figure 14 shows result of the control with the system in a temperature T = 291.15 K and forcing frequency ω = 5.5 rad/s. Initially the system presents a chaotic response. After 300 cycles, the control is turned on, and the system stabilizes at a period 6 orbit showed in Fig. 14b. The gain matrix used is given by:

$$K = \begin{bmatrix} 0 & 0 \\ 0.2 & 0 \end{bmatrix} \tag{6}$$

It is important to mention that this test is carried out neglecting cooling-heating asymmetry and temperature inertia.

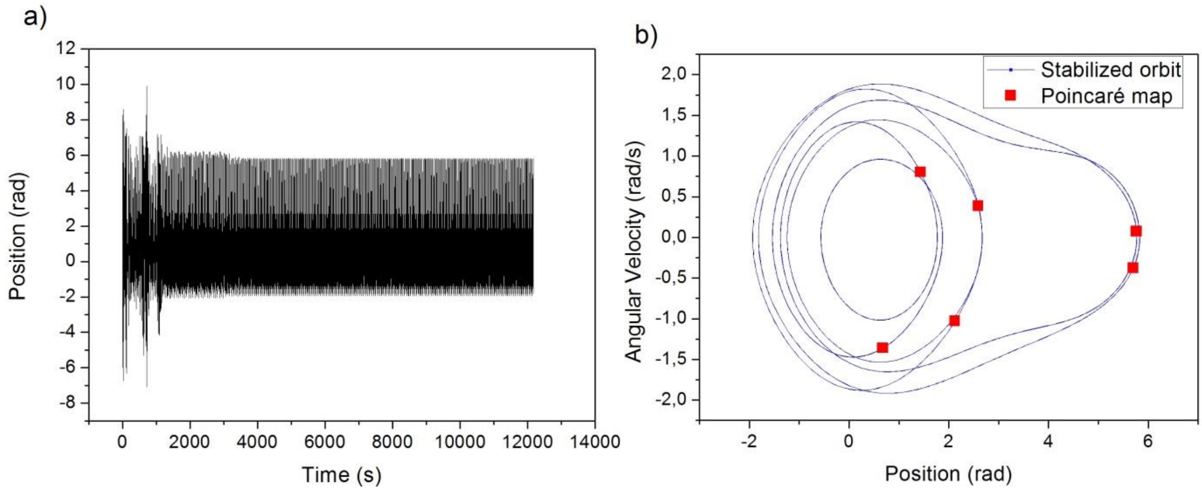

Figure 14: Time delay feedback control on a chaotic region. a) System response against time. b) Stabilized orbit.

4. CONCLUSIONS

This work deals with the nonlinear dynamics of an SMA-pendulum system. The use of SMA element provides a temperature dependent behavior introducing several possibilities related to system response. The structure of equilibrium points is discussed showing a large number of points with complex behavior altered by temperature. Concerning forced vibration, system presents several complex responses including chaos, transient chaos and high periodic orbits. All these aspects can be exploited for control purposes, as temperature variations can be employed to change either the system position or the system response in a variety of ways. A control test using delayed feedback control is carried out showing the potential application for the SMA system. For real application, the cooling-heating asymmetry as well as it temperature inertia need to be accounted.

5. ACKNOWLEDGEMENTS

The authors would like to acknowledge the support of the Brazilian Research Agencies CNPq, CAPES and FAPERJ and through the INCT-EIE (National Institute of Science and Technology - Smart Structures in Engineering) the CNPq and FAPEMIG. The Air Force Office of Scientific Research (AFOSR) is also acknowledged.

6. REFERENCES

AGUIAR, R. A. A.; SAVI, M. A.; PACHECO, P. M. C. L. Experimental and numerical investigations of shape memory alloy helical springs. **Smart Materials and Structures**, v. 19, n. 2, p. 25008, 1 fev. 2010.

DE PAULA, A. S.; SAVI, M. A.; PEREIRA-PINTO, F. H. I. Chaos and transient chaos in an experimental nonlinear pendulum. **Journal of Sound and Vibration**, v. 294, n. 3, p. 585–595, jun. 2006.

ENEMARK, S.; SANTOS, I. F.; SAVI, M. A. Modelling, Characterisation and Uncertainties of Stabilised Pseudoelastic Shape Memory Alloy Helical Springs. **Journal of Intelligent Material Systems and Structures**, 2016.

LAGOUDAS, D. C. **Shape Memory Alloys**. 1. ed. Boston, MA: Springer US, 2008. v. 1

PAIVA, A. et al. A constitutive model for shape memory alloys considering tensile–compressive asymmetry and plasticity. **International Journal of Solids and Structures**, v. 42, n. 11–12, p. 3439–3457, jun. 2005.

PYRAGAS, K. Continuous Control of Chaos by Self-Controlling Feedback. **Physics Letters A**, v. 170, p. 421–428, 1992.

WOLF, A. et al. Determining Lyapunov Exponents From a Time Series. **Physica D**, v. 16, p. 285–317, 1985.